KSME

Springer

Journal of Mechanical Science and Technology 37 (10) 2023

Original Article
DOI 10.1007/s12206-023-0908-5

Keywords:
· Control methods
· In-pipe inspection
· In-pipe robot
· Localization
· Normal force estimation
· Posture control
· Tracking algorithms

Correspondence to:
Hyun Seok Yang
hsyang@yonsei.ac.kr

Citation:
Park, J., Yang, H. (2023). Pipeline mapping with crawler-type in-pipe robot feature. Journal of Mechanical Science and Technology 37 (10) (2023) 5015~5020.
http://doi.org/10.1007/s12206-023-0908-5

Received April 12th, 2023
Revised May 16th, 2023
Accepted June 22nd, 2023

† Recommended by Editor
No-cheol Park

Pipeline mapping with crawler-type in-pipe robot feature

Jungwan Park[1] and Hyunseok Yang[2]

[1]Hyundai Motor Company Institute, Hwaseong-si, Gyunggi-do 18280, Korea, [2]School of Mechanical Engineering, Yonsei University, Seoul 80309, Korea

Abstract In-pipe robots have become popular, allowing for non-destructive testing, visual inspection, and cleaning. In-pipe inspection is crucial for maintaining pipeline integrity, but it is difficult for humans to access pipelines and perform checks. This article focuses on an in-pipe robot navigating various pipeline structures and diameters. It consists of a center module, a tracking module, and an active pantograph mechanism. The hardware components, such as the motorized gear train, screw, pantograph mechanism, springs, track module, and angular sensors, are discussed. Additionally, the control methods employed by the robot, including normal force control and posture control, are explained. Finally, the tracking algorithms used to estimate the robot's position and direction within the pipeline are presented.

1. Introduction

In-pipe inspection is a critical process for assessing and maintaining the integrity of pipelines. Due to their complex and narrow internal structures, it is challenging for humans to access pipelines and conduct inspections manually. In-pipe robots have emerged as an innovative solution for pipeline inspection, offering the ability to perform non-destructive testing, visual inspection, and cleaning [1-12]. In-pipe robots come in different configurations and are equipped with sensor systems to inspect pipes. One commonly used type is the wall-pressed crawler, which uses tracks to maneuver through pipes [1-7]. This type of robot has specific mechanisms that provide a reliable traction force, making it easier to move through vertical pipes. This feature is advantageous for in-pipe inspections.

The pipe mapping methods using robots are usually based on simultaneous localization and mapping (SLAM). SLAM is helpful in tracking a robot's trajectory, but it is challenging for in-pipe robots to obtain precise location information. Pipelines are similar in shape, making it challenging to find landmarks, and it is difficult to get external location information, such as the global positioning system (GPS), because they are mostly buried underground. Therefore, some researchers have been focused on sending location information from outside [13, 14]. Visual SLAM has also been studied widely to find landmarks using visual sensors inside or outside a pipeline [15-17]. SLAM with visual sensors also has been researched widely. Dead reckoning estimates an object's current position and orientation based on its movement without absolute location information. The inner space of a pipeline is a suitable environment for dead reckoning, so much research has been studied [18-20]. However, it is vulnerable to directional drift, which can lead to significant errors if the pipe's axial direction and the pipe robot's heading angle are not aligned.

This paper focuses on an in-pipe robot that can navigate horizontal, vertical, bent, and branched pipelines with diameters ranging from 250 to 400 mm. The robot is equipped with a center module, a track module, and an active pantograph mechanism. This chapter introduces the robot's hardware components, including the motorized gear train, screw, pantograph mechanism, springs, track module, and angular sensors. The control methods employed by the robot, namely normal force control and posture control, are also discussed. The text concludes with an overview of the tracking algorithms used to estimate the robot's position and direction

within the pipeline.

2. In-pipe robot

Fig. 1 shows the developed in-pipe robot consisting of three parts: a center module, a track module, and an active pantograph mechanism. The four pantograph mechanisms and the track modules are symmetrically located on the center module. The center and track modules are equipped with a control unit and communicate with each other via the control area network (CAN) protocol. The robot can maneuver horizontal, vertical, bent, and branched pipes with diameters ranging from 250 to 400 mm by widening and shortening the length of the pantograph mechanism.

2.1 Hardware

The center module is equipped with a motorized gear train that drives a screw having both right and left-handed threads, as shown in Fig. 2. As the motor rotates the screw, the screw nuts connected to both ends of the pantograph move closer or farther apart, thereby controlling the length of the pantograph. The pantograph mechanism moves radially, ensuring no distortion force appears while expanding or contracting the mechanism [7]. The springs are installed between the open ends of the pantographs and nut screws in the center module to provide the mechanism with compliance for uneven inner surfaces of a pipeline. The track module is attached at the closed end of the pantograph with free rotation joints and has several idle pulleys to maintain proper traction on uneven surfaces. Angular sensors are located at both ends of the pantograph to detect the angle between the pantograph's link and the center or track module.

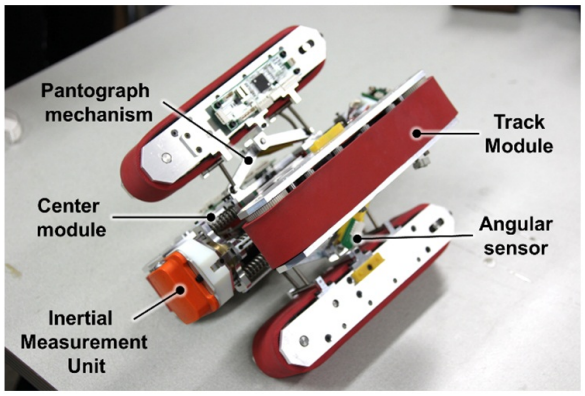

Fig. 1. The overview of developed pipe robot.

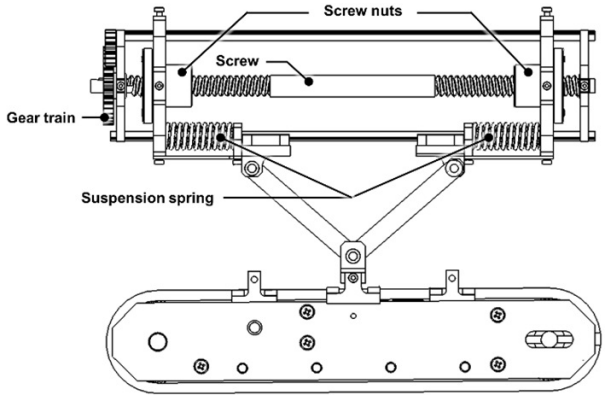

Fig. 2. The structure of center and track modules.

2.2 Control methods

The robot uses two control methods while traveling in pipelines: normal force control and posture control. Fig. 3 shows the quasi-static analysis when the track module pushes the inner wall of a pipe. The relationship between the normal force and the compression of the suspension spring in the center module is expressed by Eq. (1), where N is the normal force between the inner wall of the pipe and the track module, F_s is the spring force, and θ_l is the angle between the pantograph and the center module, which is detected by the angular sensor.

$$F_s = \frac{1}{2} N \tan\theta_l \,. \tag{1}$$

The normal force can be calculated if the compression forces of the springs are known. The position of the ends of the

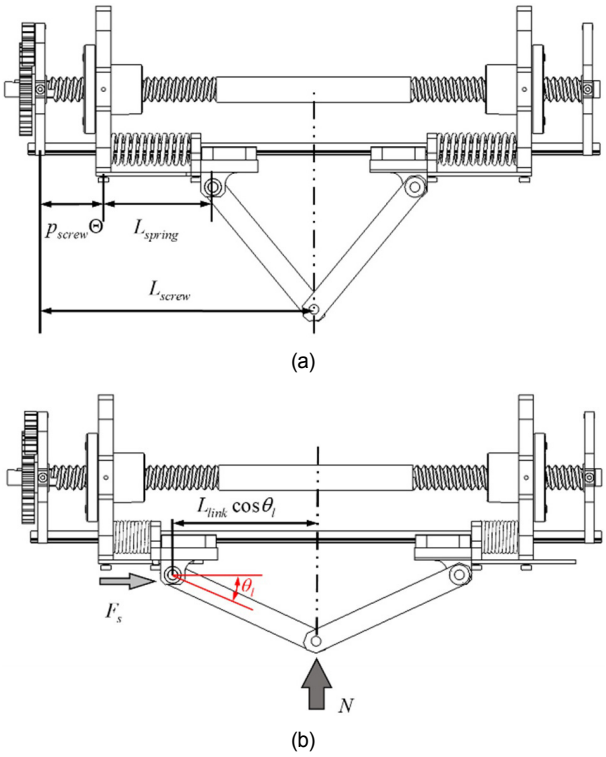

Fig. 3. Position analysis with (a) no-load; (b) load conditions.

pantograph with uncompressed springs is computed by Eq. (2), while the position with compressed springs is expressed by Eq. (3). The stiffness of the spring is known, and the normal force can be estimated by Eq. (4).

$$L_{noload} = L_{screw} - p_{screw}\Theta - L_{spring} \tag{2}$$

$$L_{load} = L_{link}\cos\theta_l \tag{3}$$

$$N = 2\cot\theta_l K_s\left(L_{screw} - p_{screw}\Theta - L_{spring} - L_{link}\cos\theta_l\right). \tag{4}$$

Here, L_{screw}, p_{screw}, and Θ are the half-length, pitch, and revolute angle of the screw, respectively. L_{spring} is the length of the spring with a no-load condition, while L_{link} is the link length of the mechanism.

For successful travel, the robot's heading direction should align with a pipeline's axial direction. If the directions are not aligned, the robot may lose the proper posture for traveling and could be unable to move. Fig. 4 illustrates the posture of the robot when it is misaligned with the axial direction of a pipe. Although the robot's pose is misaligned, the track modules maintain contact because they rotate freely about the pantograph mechanism. The rotation angle of the track module, θ_t, is detected by the angular sensor attached to the closed end of the mechanism. Fig. 5 shows the schematic of posture control. All the track module rotation angles are compared with the average angle and increase or decrease each track's velocity to maintain the same angle and proper posture. This method ensures that the robot stays aligned with the axial direction of the pipe and can maneuver in pipelines, including shrink or expanding pipes, without preliminary information.

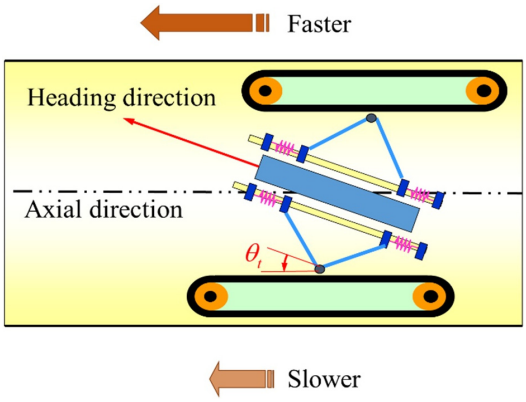

Fig. 4. The concept of the posture control.

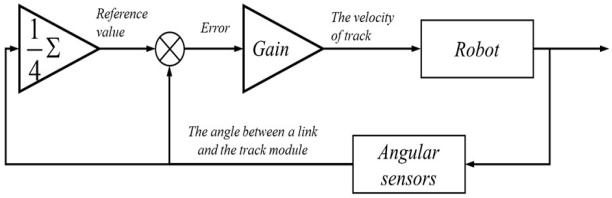

Fig. 5. The block diagram of posture control.

3. Tracking algorithms

Dead reckoning is an estimation method to determine a moving object's current orientation and position. As most pipelines are buried underground, and it is difficult to obtain global position data, the dead reckoning system is usually used to estimate the trajectory of an in-pipe robot. However, dead reckoning is vulnerable to directional drift. Since the robot can travel misaligned with the direction of a pipe, directional drift can occur, and estimated errors caused by the drift could increase with the traveled distance. Therefore, detecting the axial direction of a pipeline is necessary to reduce the effect of the drift.

If a coordinate system with the robot's center of gravity as the origin is set, as shown in Fig. 6, the speed of each track and the rate of change in the robot's direction can be expressed as follows. Hence, the Jacobian of the robot can be defined as Eq. (5).

$$\begin{bmatrix}\dot{x}\\ \dot{y}\\ \dot{z}\\ \dot{\alpha}\\ \dot{\beta}\\ \dot{\gamma}\end{bmatrix} = \begin{bmatrix} \frac{1}{4}\cos\theta_{t1} & \frac{1}{4}\cos\theta_{t2} & \frac{1}{4}\cos\theta_{t3} & \frac{1}{4}\cos\theta_{t4} \\ -\frac{1}{4}\sin\theta_{t2} & 0 & \frac{1}{4}\sin\theta_{t3} & 0 \\ 0 & -\frac{1}{4}\sin\theta_{t2} & 0 & \frac{1}{4}\sin\theta_{t4} \\ 0 & 0 & 0 & 0 \\ \frac{\cos\theta_{t1}}{4L_1} & 0 & -\frac{\cos\theta_{t3}}{4L_3} & 0 \\ 0 & \frac{\cos\theta_{t2}}{4L_2} & 0 & -\frac{\cos\theta_{t4}}{4L_4} \end{bmatrix} \begin{bmatrix} v_1\\ v_2\\ v_3\\ v_4\end{bmatrix} = \begin{bmatrix}\mathbf{J}_T\\ \mathbf{J}_A\end{bmatrix}\mathbf{V}. \tag{5}$$

Here, x, y, and z are translations along with each axis. α, β and γ are the angles rotated around the X, Y and Z axes, respectively. v is the velocity of a track module,

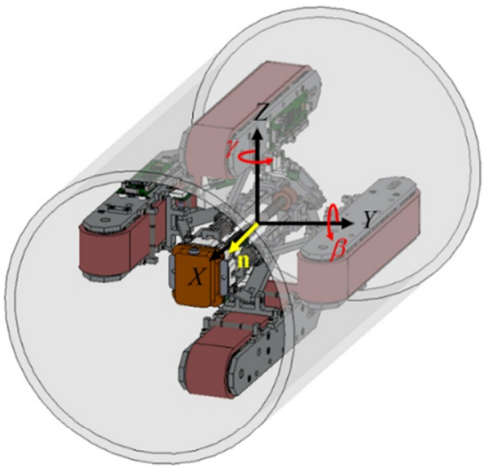

Fig. 6. The coordinate system on the robot.

L is the length from the center of the robot to a track module, and the subscription implies the number of each track module. The matrices $\mathbf{J}_T$ and $\mathbf{J}_A$ are Jacobian about translation and angular motion.

Assuming no obstacles are inside the pipe, the front and rear pulleys of the track module are always in contact with the pipe's inner wall. If a cylinder that passes through the location of all the contact points can be found, information about the pipe can be obtained. However, the number of cylinders passing through the designated points in space is so large that finding one cylinder defining the current pipe is impossible [21]. Therefore, the actual location and direction of the pipe are estimated through simple assumptions. It is assumed that the orientation of the pipe is rotated around the Y axis and Z axis in the coordinate system. This assumption is valid because the pipe is cylindrical, so it can be ignored to turn around the X axis. Since the robot's track modules are located 90 degrees apart around the center module, those exist on the axis of the coordinate system, and rotation for each axis will be reflected in the rotation angles of the track modules. The axial direction of the pipe can be assumed as follows:

$$\hat{\beta} = \frac{1}{2}(\theta_{t3} - \theta_{t1}) \tag{6}$$

$$\hat{\gamma} = \frac{1}{2}(\theta_{t2} - \theta_{t4}) \tag{7}$$

$$n = \left[\cos\beta\cos\gamma \quad \sin\gamma \quad -\sin\beta\cos\gamma\right]^T. \tag{8}$$

$\mathbf{n}$ is the axial direction of the pipe, and notation T means the transpose. Since the robot's movement will take place along the $\mathbf{n}$, the acceleration of the robot must also be equal to the vector $\mathbf{n}$. Let the state vector be denoted as $\mathbf{X}$, according to Eq. (9). Vector $\mathbf{p}$, $\mathbf{v}$, $\mathbf{a}$, $\mathbf{q}$, $\boldsymbol{\omega}$, and $\mathbf{b}$ represent the position, velocity, acceleration, rotation angle, the angular velocity of the robot, and bias of the accelerometer, respectively. The state space equations are given by Eqs. (10) and (11), where $\mathbf{F}$, $\mathbf{J}$, $\boldsymbol{\Gamma}$, and $\mathbf{H}$ represent the system, input, disturbance input, and output matrices, respectively. The disturbance, jerk, is expressed as $\mathbf{j}$. The matrices are determined as Eqs. (12)-(15). $[\times]$ is the notation for Rodrigues' formula.

$$\mathbf{X}_k = \left[\mathbf{p}_k^T \quad \mathbf{v}_k^T \quad \mathbf{a}_k^T \quad \mathbf{b}_k^T \quad \mathbf{q}_k^T \quad \boldsymbol{\omega}_k^T\right] \tag{9}$$

$$\mathbf{X}_{k+1} = \mathbf{F}_k\mathbf{X}_k + \mathbf{J}_k\mathbf{V}_k + \boldsymbol{\Gamma}\mathbf{j}_k \tag{10}$$

$$\mathbf{z}_{k+1} = \mathbf{H}_k\mathbf{X}_k \tag{11}$$

$$\mathbf{F}_k = \begin{bmatrix} \mathbf{I}_{3\times3} & t_s\mathbf{I}_{3\times3} & \frac{t_s^2}{2}\mathbf{I}_{3\times3} & \mathbf{0}_{3\times3} & \mathbf{0}_{3\times3} & \mathbf{0}_{3\times3} \\ \mathbf{0}_{3\times3} & \mathbf{I}_{3\times3} & t_s\mathbf{I}_{3\times3} & \mathbf{0}_{3\times3} & \mathbf{0}_{3\times3} & \mathbf{0}_{3\times3} \\ \mathbf{0}_{3\times3} & \mathbf{0}_{3\times3} & \mathbf{I}_{3\times3} & -[\mathbf{a}_k\times] & \mathbf{0}_{3\times3} & \mathbf{0}_{3\times3} \\ \mathbf{0}_{3\times3} & \mathbf{0}_{3\times3} & \mathbf{0}_{3\times3} & \mathbf{I}_{3\times3} & \mathbf{0}_{3\times3} & \mathbf{0}_{3\times3} \\ \mathbf{0}_{3\times3} & \mathbf{0}_{3\times3} & \mathbf{0}_{3\times3} & \mathbf{0}_{3\times3} & \mathbf{I}_{3\times3} & t_s\mathbf{I}_{3\times3} \\ \mathbf{0}_{3\times3} & \mathbf{0}_{3\times3} & \mathbf{0}_{3\times3} & \mathbf{0}_{3\times3} & \mathbf{0}_{3\times3} & [\boldsymbol{\omega}_k\times] \end{bmatrix} \tag{12}$$

$$\mathbf{J}_k = \begin{bmatrix} [\boldsymbol{\omega}_k\times]\mathbf{J}_{Tk} \\ \mathbf{0}_{3\times4} \\ \mathbf{0}_{3\times4} \\ \mathbf{0}_{3\times3} \\ [\boldsymbol{\omega}_k\times]\mathbf{J}_{Ak\,3\times4} \\ \mathbf{0}_{3\times3} \end{bmatrix} \tag{13}$$

$$\boldsymbol{\Gamma}_k = \begin{bmatrix} \frac{t_s^3}{6}\mathbf{I}_{3\times3} \\ \frac{t_s^2}{2}\mathbf{I}_{3\times3} \\ t_s\mathbf{I}_{3\times3} \\ \mathbf{0}_{3\times3} \\ \mathbf{0}_{3\times3} \\ \mathbf{0}_{3\times3} \end{bmatrix} \tag{14}$$

$$\mathbf{H}_k = \begin{bmatrix} \mathbf{0}_{3\times3} & \mathbf{0}_{3\times3} & \mathbf{n}\left(\mathbf{n}^T\mathbf{I}_{3\times3}\right) & \mathbf{0}_{3\times3} & \mathbf{0}_{3\times3} & \mathbf{0}_{3\times3} \\ \mathbf{0}_{3\times3} & \mathbf{0}_{3\times3} & \mathbf{0}_{3\times3} & \mathbf{0}_{3\times3} & \mathbf{0}_{3\times3} & \mathbf{I}_{3\times3}[\boldsymbol{\omega}\times] \end{bmatrix}. \tag{15}$$

4. Experiments

Fig. 7 illustrates the test bed, consisting of straight and 90-degree bent pipes. An IMU attached to the pipeline's center detects the robot's accelerations and rotations. Figs. 8 and 9 depict the estimated trajectory of the robot without and with modified acceleration, respectively, assuming the axial direc-

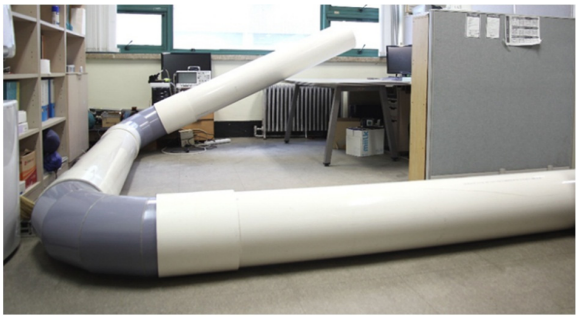

Fig. 7. The experimental pipeline.

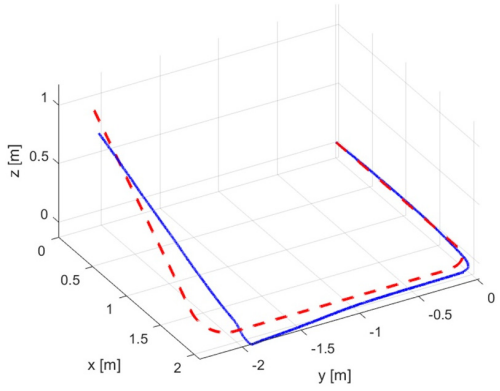

Fig. 8. The estimated trajectory using pure dead reckoning.

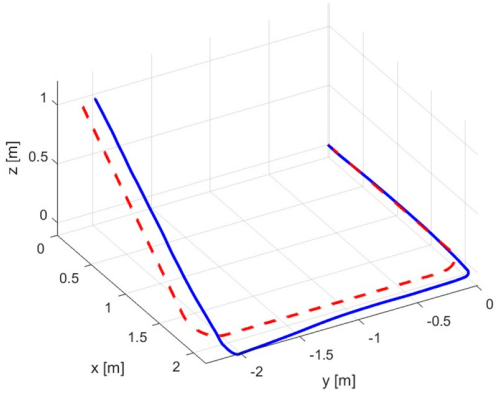

Fig. 9. The estimated trajectory with modified acceleration.

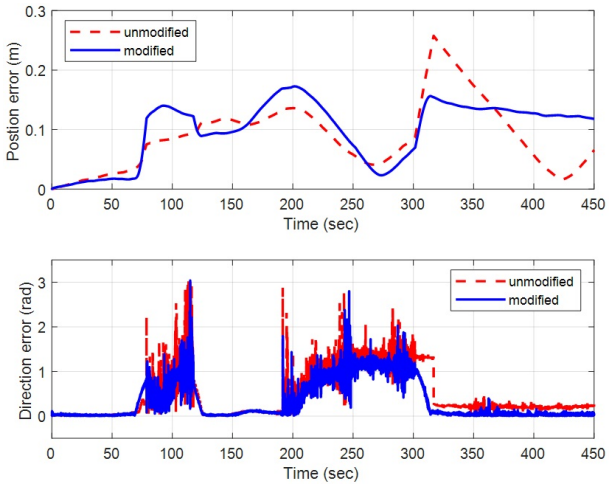

Fig. 10. Position and direction error.

tion of a pipe. Fig. 10 shows the position and direction error between the pipe and the estimated trajectories. The position error's root mean square (RMS) increased from 15.89 to 16.73. This indicates that the method's position estimation without using the corrected acceleration value crossed the actual position, resulting in improved error. The RMS of the directional error has significantly reduced from 109.62 to 87.26. Considering that the effectiveness of directional drift increases with the travel distance, estimating from pipelines longer than the experimental environment can lead to significant improvements in estimation accuracy.

5. Conclusions

In this paper, we explained how to control robots that can pass through pipes of various shapes and sizes and suggested ways to improve the path estimation method by obtaining the robot's Jacobian and estimating the pipe's direction. We proved through experiments that there was a slight improvement even in a short pipeline due to space constraints. Considering that the error accumulation by drift increases with longer travel distances, the results of this paper are expected to contribute to improving the estimation of the trajectory of an in-pipe robot.

References

[1] J. Park, D. Hyun, W.-H. Cho, T.-H. Kim and H.-S. Yang, Normal-force control for an in-pipe robot according to the inclination of pipelines, *IEEE Trans. Industrial Electronics*, 58 (12) (2011) 5304-5310.

[2] S. Roh and H. R. Choi, Differential-drive in-pipe robot for moving inside urban gas pipelines, *IEEE Trans. Robotics*, 21 (1) (2005) 1-17.

[3] Y.-S. Kwon and B.-J. Yi, Design and motion planning of a two-module collaborative indoor pipeline inspection robot, *IEEE Trans. Robotics*, 28 (3) (2012) 681-696.

[4] Y. Zhang and G. Yan, In-pipe inspection robot with active pipe-diameter adaptability and automatic tractive force adjusting, *Mechanism and Machine Theory*, 42 (12) (2007) 1618-1631.

[5] H. Schempf, E. Mutschler, A. Gavaert, G. Skoptsov and W. Crowley, Visual and nondestructive evaluation inspection of live gas mains using the Explorer™ family of pipe robots, *Journal of Field Robotics*, 27 (3) (2010) 217-249.

[6] D. Lee, J. Park, D. Hyun, G. Yook and H. Yang, Novel mechanisms and simple locomotion strategies for an in-pipe robot that can inspect various pipe types, *Mechanism and Machine Theory*, 56 (2012) 52-68.

[7] I. N. Ismail, A. Anuar, K. S. M. Sahari, M. Z. Baharuddin, M. Fairuz, A. Jalal and J. M. Saad, Development of in-pipe inspection robot: A review, *2012 IEEE Conf. Sustainable Utilization and Development in Engineering and Technology*, Kuala Lumpur, Malaysia (2012) 310-315.

[8] W. Jeon, I. Kim, J. Park and H. Yang, Design and control method for a high-mobility in-pipe robot with flexible links, *Industrial Robot*, 40 (3) (2013) 261-274.

[9] T. Oya and T. Okada, Development of a steerable, wheel-type, in-pipe robot and its path planning, *Advanced Robotics,* 19 (6) (2005) 635-650.

[10] Y. Nakazato, Y. Sonobe and S. Toyama, Development of an In-pipe micro mobile robot using peristalsis motion, *Journal of Mechanical Science and Technology,* 24 (2010) 51-54.

[11] H. Lu, J. Zhu, Z. Lin and Y. Guo, An inchworm mobile robot using electromagnetic linear actuator, *Mechatronics*, 19 (7) (2009) 1116-1125.

[12] C. Choi, B. Park and S. Jung, The design and analysis of a feeder pipe inspection robot with an automatic pipe tracking system, *IEEE/ASME Trans. Mechatronics*, 15 (5) (2010) 736-745.

[13] H. Qi, X. Zhang, H. Chen and J. Ye, Tracing and localization system for pipeline robot, *Mechatronics*, 19 (1) (2009) 76-84.

[14] H. Qi, J. Ye, X. Zhang and H. Chen, Wireless tracking and locating system for in-pipe robot, *Sensors and Actuators A: Physical*, 159 (1) (2010) 117-125.

[15] H. Lim, J. Y. Choi, Y. S. Kwon, E.-J. Jung and B.-J. Yi, SLAM in indoor pipelines with 15 mm diameter, *IEEE Int. Conf. Robotics and Automation*, Pasadena, CA, USA (2008) 4005-4011.

[16] D. Y. Kim, J. Kim, I. Kim and S. Jun, Artificial landmark for vision-based slam of water pipe rehabilitation robot, *12th Int.*

Conf. Ubiquitous Robots and Ambient Intelligence, Goyangi, Korea (2015) 444-446.

[17] P. Hansen, H. Alismail, B. Browning and P. Rander, Stereo visual odometry for pipe mapping, *IEEE/RSJ Int. Conf. Intelligent Robots and Systems*, San Francisco, CA, USA (2011) 4020-4025.

[18] A. C. Murtra and J. M. Mirats Tur, IMU and cable encoder data fusion for in-pipe mobile robot localization, *IEEE Conf. Technologies for Practical Robot Applications*, Woburn, MA, USA (2013) 1-6.

[19] D. Hyun, H. S. Yang, H.-S. Park and H.-J. Kim, Dead-reckoning sensor system and tracking algorithm for 3-D pipeline mapping, *Mechatronics*, 20 (2) (2010) 213-223.

[20] D. Hyun, H. S. Yang, H. R. Park and H.-S. Park, Differential optical navigation sensor for mobile robots, S*ensors and Actuators A: Physical*, 156 (2) (2009) 296-301.

[21] O. Devillers, B. Mourrain, F. P. Preparata and P. Trebuchet, Circular cylinders through four or five points in space, *Discrete and Computational Geometry*, 29 (2003) 83-104.

Jungwan Park is the Senior Engineer in the Commercial Vehicle Division, at Hyundai Motors. He received the B.S. and Ph.D. degrees in the School of Mechanical Engineering, Yonsei University, Seoul, Korea, in 2008 and 2016, respectively. His research interests the robotics and motion control.

Hyunseok Yang received a B.S. degree from Yonsei University, Seoul, Korea, in 1984 and the M.S. and Ph.D. in mechanical engineering from the Massachusetts Institute of Technology, Boston, in 1988 and 1993, respectively. Since 1994, he has been with Yonsei University, Seoul, Korea, where he is currently a Professor in the School of Mechanical Engineering. His research interests include robotics and motion control.